J|A|C|S
COMMUNICATIONS

Isolable Photoreactive Polysilyl Radicals

Gregory Molev, Boris Tumanskii,* Dennis Sheberla, Mark Botoshansky, Dmitry Bravo-Zhivotovskii,
and Yitzhak Apeloig*

*Schulich Faculty of Chemistry and the Lise Meitner Minerva Center for Computational Quantum Chemistry,
Technion-Israel Institute of Technology, Haifa 32000, Israel*

Received June 21, 2009; E-mail: tboris@tx.technion.ac.il; apeloig@tx.technion.ac.il

Silyl radicals play an important role in many fields of chemistry.[1] For example, in organic synthesis they efficiently abstract halogen atoms from organic halides,[1g] they are used as catalysts in cyclotrimerization of acetylenes,[1h] etc.[1] Silyl radicals are also intermediates in the synthesis and photodegradation of polysilanes, an important class of polymers.[2] Similarly to polysilanes,[2c−g] polysilyl radicals may also be photoreactive,[3] but their photoreactivity was not studied because isolable silyl radicals were not available until 2002, when $(t\text{-Bu}_2\text{MeSi})_3\text{Si}\bullet$, the first isolable silyl radical lacking conjugation with π-bonds, was reported.[4] However, its photoreactivity was not reported. The synthesis and isolation of new silyl radicals, in particular stable ones, remain a synthetic challenge, which when achieved will result in a better understanding of the properties, reactivity, and possible applications of these important species.

In this paper we report the synthesis, isolation, and photoreactivity of two stable silyl radicals, the new $(t\text{-Bu}_2\text{MeSi})_2\text{HSi}(t\text{-Bu}_2\text{MeSi})_2\text{Si}\bullet$ (**1**) and the previously known $(t\text{-Bu}_2\text{MeSi})_3\text{Si}\bullet$ (**2**).[4] *Both radicals were synthesized in high yield using a new one step method* (eq 1), which is general and can be applied for the synthesis of other stable radicals. This is the first report on the photochemistry of silyl radicals.

Radical **1** was synthesized by a one-step reaction of the corresponding silyl substituted dichlorosilane **A** with $t\text{-Bu}_2\text{MeSiLi}$ (**B**)[5] (eq 1). **1** was isolated as orange crystals (Figure 1a, left insert) in 65% yield by crystallization of the reaction mixture from hexane. Radical $(t\text{-Bu}_2\text{MeSi})_3\text{Si}\bullet$ (**2**)[4] was obtained similarly (eq 1) in 85% yield.[6] The molecular structures of radicals **1** and **2** were determined by X-ray crystallography as well as by EPR spectroscopy. The method in eq 1 was used successfully to synthesize several other silyl and aryl substituted silyl radicals.[7] Thus, eq 1 presents a straightforward general method for the synthesis of silyl radicals.

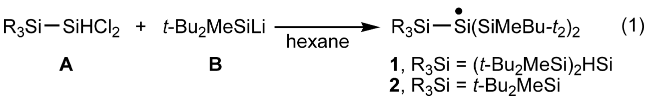

$$\underset{\textbf{A}}{\text{R}_3\text{Si}-\text{SiHCl}_2} + \underset{\textbf{B}}{t\text{-Bu}_2\text{MeSiLi}} \xrightarrow[\text{hexane}]{} \text{R}_3\text{Si}-\overset{\bullet}{\text{Si}}(\text{SiMeBu-}t_2)_2 \qquad (1)$$

1, $\text{R}_3\text{Si} = (t\text{-Bu}_2\text{MeSi})_2\text{HSi}$
2, $\text{R}_3\text{Si} = t\text{-Bu}_2\text{MeSi}$

The molecular structure of **1** (given in the Supporting Information, Figure S1) could be determined only at low resolution ($R = 0.15$) due to the low quality of the crystals, and therefore its accurate structural parameters could not be obtained, but its structure is definitely that of **1**, as is also fully supported by its reactions. Thus, oxidation of **1** with HgF_2 yields $(t\text{-Bu}_2\text{MeSi})_2\text{HSi}(t\text{-Bu}_2\text{MeSi})_2\text{SiF}$ (**1a**) (Scheme 1, path a), and reduction with lithium metal in hexane or with $t\text{-Bu}_2\text{MeSiLi}$ in THF quantitatively yields $(t\text{-Bu}_2\text{MeSi})_2\text{HSi}(t\text{-Bu}_2\text{MeSi})_2\text{SiLi}$ (**1b**) (Scheme 1, path b). The structure of **1b**•4THF was determined by X-ray crystallography (R = 0.07).[8] **1** was also obtained (as verified by EPR) by low-yield methods, i.e., by oxidation of **1b** with GeCl_2 (Scheme 1, path c) and by hydrogen abstraction from silane **1c** (Scheme 1, path d).

Scheme 1

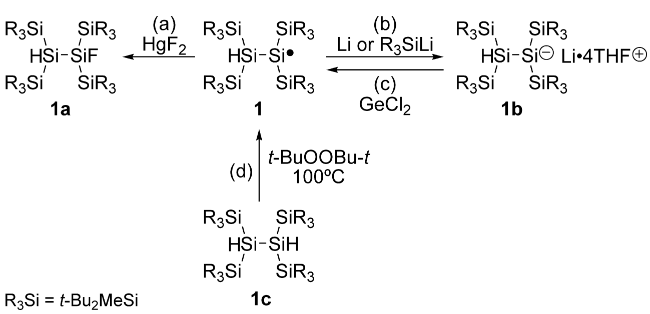

The EPR spectra of **1** in hexane solution shown in Figure 1a (EPR spectrum of the crystal is shown in the right insert) exhibits the expected splitting with the α, β, and γ Si atoms of 59.3, 7.3, and 10.4 G, respectively (^{29}Si, $I = {}^1/_2$, natural abundance 4.7%).[1b,2d,4,9] Comparison with the EPR spectrum of the nonisolable $(i\text{-Pr}_3\text{Si})_2\text{HSi}(i\text{-Pr}_3\text{Si})_2\text{Si}\bullet$ (**3**),[10] which also has a β-hydrogen (Figure 1b), is particularly insightful. The values of the g-factor and the hyperfine coupling constants (*hfc*) of the unpaired electron with the $^{29}\text{Si}^{\alpha}$ and $^{29}\text{Si}^{\beta}$ nuclei in **1** and **3** are typical for planar silyl radicals.[1b,2d,4] The EPR spectrum of **3** exhibits a doublet arising from coupling with the β-hydrogen atom, a doublet which is missing in **1**. Theoretically, the degree of splitting by H^{β} depends on the angle θ between the $\text{H}^{\beta}-\text{Si}^{\beta}$ bond and the principal axis of the 3p-orbital occupied by the unpaired electron (Figures 2a and 2b) according to eq 2, where B_0 and B are constants.[11] $a(\text{H}^{\beta})$ can, therefore, serve as a sensitive probe for the conformation of silyl radicals.[12] Comparison of the EPR spectra of radicals **1** and **3** (Figure 1) implies that they have different conformations. In **3**, $a(\text{H}^{\beta}) = 1.1$ G and therefore $\theta \neq 90°$ (Figure 2b). In contrast, in **1** where doublet splitting is not observed ($a(\text{H}^{\beta}) \leq 0.4$ G), we deduce that θ is close to 90° (Figure 2a).

$$a(\text{H}^{\beta}) = B_0 + B\cos^2\theta \qquad (2)$$

DFT calculations[13] support the conformations proposed in Figure 2 for **1** and **3**. Thus, according to the DFT calculations in **1** $\theta = 82.0°$ and there is no spin density on H^{β}, while in **3** $\theta = 63°$ and some spin density resides on H^{β} (Figure 2c and 2d, respectively). In line with these conformations, calculations also show spin-density transfer by hyperconjugation to the Si^{γ} and H^{β} nuclei,[11] as indicated by the positive spin density (yellow area in Figure 2c and 2d). In contrast, spin-density transfer to Si^{β} occurs by a spin-polarization mechanism,[11] as indicated by the negative spin density (blue area in Figure 2c and 2d). The different mechanisms of the spin-density transfer explain the fact that in **1** and **3** $a(^{29}\text{Si}^{\gamma})$ is larger than $a(^{29}\text{Si}^{\beta})$.[11,14]

By solving eq 2, using the observed $a(\text{H}^{\beta})$ and the calculated angles θ, parameters B and B_0 were calculated to be $B_0 \approx 0$ G,

10.1021/ja905097b CCC: $40.75 © 2009 American Chemical Society

$B = 5.4$ G. Thus, *the maximum value ($\theta = 0°$) of $a(H^{\beta})$ in branched polysilyl radicals of type* **1** *is ~5.4 G.*

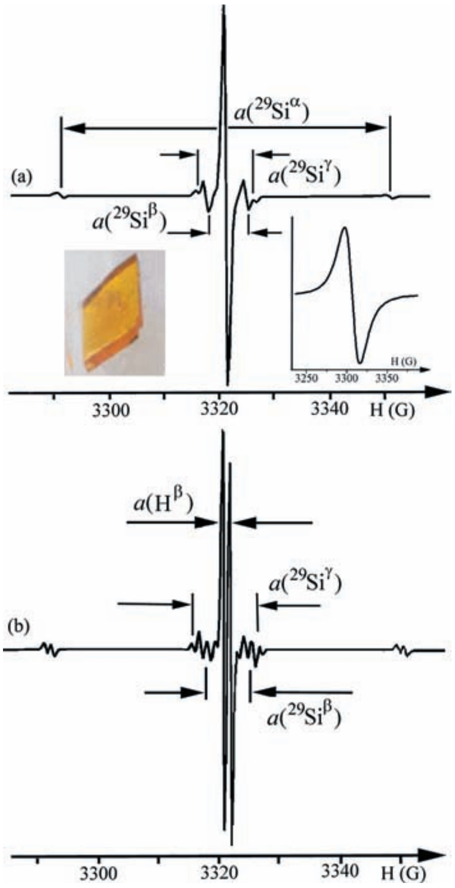

Figure 1. (a) EPR spectrum of **1** (290 K, hexane) [$a(^{29}\text{Si}^{\alpha}) = 59.3$ G; $a(3^{29}\text{Si}^{\beta}) = 7.3$ G; $a(^{29}\text{Si}^{\gamma}) = 10.4$ G; $g = 2.0051$]; left insert: crystal of **1**; right insert: EPR spectrum of the crystal of **1**; (b) EPR spectrum of **3** (290 K, hexane) [$a(^{29}\text{Si}^{\alpha}) = 57.13$ G; $a(3^{29}\text{Si}^{\beta}) = 7.5$ G; $a(H^{\beta}) = 1.12$ G, $a(^{29}\text{Si}^{\gamma}) = 10.0$ G, $g = 2.0054$].

When a hexane solution of **1** is exposed to sunlight for 2 days its color changes from yellow to deep blue and EPR spectroscopy shows no signal of **1**, indicating its full conversion. NMR analysis of the reaction mixture showed two major products: 1,2-dihydridisilane **1c** (~40%) and the blue-colored disilene **4**[15] (~40%) (Scheme 2). This interesting reaction may proceed *via* two conceivable pathways: (a) disproportionation of two molecules of **1** (i.e., upon irradiation one molecule of **1** abstracts a β-hydrogen from a second molecule of **1** (Scheme 2, path a)) or (b) cleavage of the central Si−Si bond of **1** to produce the α-H radical **5** and silylene **6** which dimerize to produce **1c** and **4**, respectively (Scheme 2, path b).

To gain insight into the mechanism of this reaction, **1** was reacted with an excess of triethylsilane or of 2-propanol, which are known to effectively trap silylenes of type **6**.[16] In the dark no reaction occurs and **1** remains intact. However, upon sunlight irradiation for 1 h full conversion of **1** is observed. The major product is **1c**, i.e., resulting from hydrogen abstraction by **1** from triethylsilane or 2-propanol. Neither disilene **4** nor trapping products of a silylene, such as $(R_3Si)_2HSiOPr$-*i* (in reaction with 2-propanol), are formed. Based on these experiments we suggest that the photoreactivity of **1** is due to its β-hydrogen, which is abstracted by a photoexcited **1**, i.e., *via* the disproportionation mechanism shown in Scheme 2, path a. The disproportionation mechanism is also supported by the observed second-order decay of the EPR signal of **1** upon irradiation, pointing to a bimolecular reaction.[17]

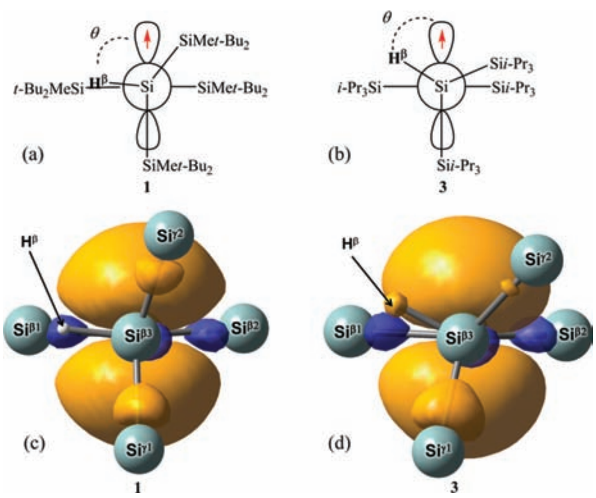

Figure 2. DFT calculated: Newman projections of (a) **1**; (b) **3** and spin densities at the 0.001 au contour level of (c) **1** and (d) **3**. The yellow and blue areas correspond to regions of positive and negative spin density, respectively. Carbon and hydrogen atoms (except H$^{\beta}$) were omitted for clarity.

Scheme 2

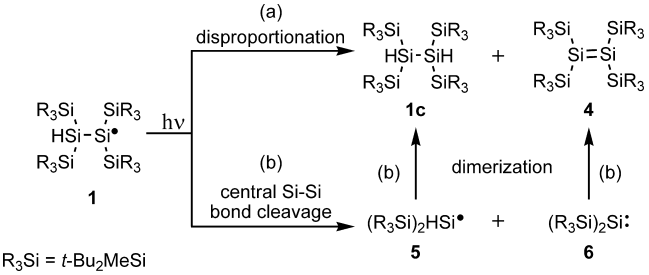

To further test this hypothesis, radical **2**, lacking a β-hydrogen and which is photostable in the absence of additives, was reacted in hexane with an excess of silane **1c** within the EPR spectrometer cavity. **1c** was chosen as the hydrogen source because its structure is very similar to that of **1**, and because it does not absorb at $\lambda >$ 400 nm, and therefore it is not photoreactive under these conditions. In the dark no decay of radical **2** was observed in the presence of **1c**. However, upon irradiation with a 1 kW mercury lamp at $\lambda >$ 400 nm, **2** decayed rapidly ($\tau_{1/2} \approx 100$ s) yielding $(t\text{-Bu}_2\text{MeSi})_3\text{SiH}$ (**2a**) as the major product. Upon irradiation **2** reacts also with 2-propanol and triethylsilane to yield **2a** as the major product. These photoreactions of **2** with **1c**, Et_3SiH, and *i*-PrOH support our conclusion that **1** reacts photochemically *via* disproportionation (Scheme 2, path a).

Why are radicals **1** and **2** photoreactive? The two lowest energy absorption bands in radical **1** are at 350 nm ($\epsilon = 3360$) and at 428 nm ($\epsilon = 800$) (Figure 3a) and in radical **2**[4] at 303 nm ($\epsilon = 1300$) and 421 nm ($\epsilon = 100$). TD-DFT calculations[13] show that excitation of radicals **1** and **2** with $\lambda > 400$ nm causes a SOMO-1 → SOMO transition (Figure 3b).[18] This excitation creates a hole in the SOMO-1 orbital (Figure 3c), enhancing the electron-acceptor capability of the radicals.[18,19]

The proposed stepwise mechanism for the photoreaction of radical **1** is shown in Scheme 3. First, the radical undergoes photoexcitation (Scheme 3, path a) and then the photoexcited radical accepts an electron from another radical, forming within a solvent

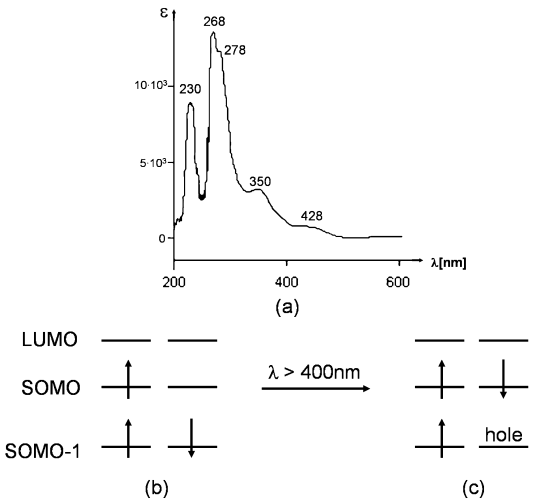

Figure 3. (a) UV−vis spectrum of radical **1** (hexane, 300 K, quartz vacuum cuvette). (b, c) Schematic representation of the molecular orbitals of radicals **1** and **2** in (b) the ground state and (c) in the SOMO-1 → SOMO excited state.

cage an ion pair (Scheme 3, path b), followed by proton transfer from the cation to the anion (Scheme 3, path c).[18,20]

Scheme 3

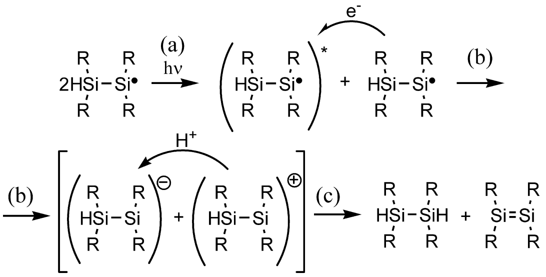

In summary, we discovered a new single-step general method for the synthesis of isolable silyl radicals and studied their photoreactions. We continue to explore the synthesis of other stable silyl radicals and to study their chemistry.

Acknowledgment. Dedicated to Professor Josef Michl on the occasion of his 70th birthday. This research was supported by the Israel Science Foundation, the Minerva Foundation in Munich and USA-Israel Binational Science Foundation (BSF). M.B., B.T., and D.B.-Z. are grateful to the Ministry of Immigrant Absorption for fellowships. The authors thank Dr. Monica Kosa for help in calculations and for fruitful discussions.

Supporting Information Available: CIF files of the X-ray structures, the syntheses and spectroscopic data for all new compounds, calculation details, Figures S1−S9, and complete ref 13. This material is available free of charge via the Internet at http://pubs.acs.org.

References

(1) (a) Lee, V. Ya.; Nakamoto, M.; Sekiguchi, A. *Chem. Lett.* **2008**, *37*, 128. (b) Sekiguchi, A.; Lee, V. Ya. *Eur. J. Inorg. Chem.* **2005**, 1209. (c) Chatgilialoglu, C. *Organosilanes in Radical Chemistry*; Wiley: Chichester, U.K., 2004. (d) Power, P. *Chem. Rev.* **2003**, *103*, 789. (e) Lee, V. Ya.; Sekiguchi, A. *Acc. Chem. Res.* **2007**, *40*, 410. (f) Lee, V. Ya.; Sekiguchi, A. In *Reviews of Reactive Intermediates Chemistry*; Moss, R. A., Platz, M. S., Jones, M., Jr., Eds.; Wiley: Hoboken, NJ, 2007. (g) Chatgilialoglu, C. *Chem.—Eur. J.* **2008**, *14*, 2310. (h) Zhu, Z. Y.; Wang, C. F.; Xiang, X.; Pi, C. F.; Zhou, X. G. *Chem. Commun.* **2006**, 2066.

(2) (a) Birot, M.; Pillot, J.-P.; Dunogues, J. *Chem. Rev.* **1995**, *95*, 1443. (b) Luh, T. Y.; Cheng, Y. J. *Chem. Commun* **2006**, 4669. (c) Kravchenko, V.; Bravo-Zhivotovskii, D.; Tumanskii, B.; Botoshansky, M.; Segal, N.; Molev, G.; Kosa, M.; Apeloig, Y. In *Organosilicon Chemistry VI: From Molecules to Materials*; Auner, N., Weis, J., Eds.; Wiley-VCH: Weinheim, 2005; p 48. (d) Kira, M.; Badugu, R. In *Handbook of Photochemistry and Photobiology*; Nalwa, H. S., Ed.; American Scientific Publishers: Stevenson Ranch, CA, 2003; Vol. 1. (e) Fogarty, H. A.; Casher, D. L.; Imhof, R.; Schepers, T.; Rooklin, D. W.; Michl, J. *Pure Appl. Chem.* **2003**, *75*, 999. (f) Apeloig, Y.; Bravo-Zhivotovskii, D.; Yuzefovich, M.; Bendikov, M.; Shames, A. *Appl. Magn. Reson.* **2000**, *18*, 425. (g) Azinovic, D.; Bravo-Zhivotovskii, D.; Bendikov, M.; Apeloig, Y.; Tumanskii, B.; Veprek, S. *Chem. Phys. Lett.* **2003**, 257.

(3) Photochemistry of stable organic radicals was reported. Canepa, M.; Fox, M. A.; Whitesell, J. K. *J. Org. Chem.* **2001**, *66*, 3886.

(4) Sekiguchi, A.; Fukawa, T.; Nakamoto, M.; Lee, V.Ya.; Ichinohe, M. *J. Am. Chem. Soc.* **2002**, *124*, 9865.

(5) Synthesis of **1**: a hexane solution (4 mL) of t-Bu$_2$MeSiLi (**B**) (0.5 g, 3.0 mmol) was added to a frozen hexane solution (10 mL) of (t-Bu$_2$MeSi)$_2$HSiSiHCl$_2$ (**A**) (0.44 g, 1.0 mmol). The frozen mixture was warmed up to 0 °C and stirred for 1 h in the dark. All volatile compounds were then evaporated in vacuum, and 5 mL of dry hexane were added. Keeping the solution at−30°C for 12 h yielded 0.45 g (65%) of orange prisms (Figure 1a, insert) identified as **1** by X-ray crystallography (Figure S1), EPR spectroscopy (Figure 1a), trapping reactions (Scheme 1, paths a, b), and non-preparative synthesis from other precursors (Scheme 1, paths c, d); UV−vis (Figure 3a): 230 nm (9300), 268 nm (13130), 278 nm (12200), 350 nm (3360), 428 nm (800).

(6) Radical **2** was obtained previously in 44% yield.[4] The EPR spectra of **2** at high resolution and in toluene glass (not reported previously) are given in Figures S5 and S6, respectively.

(7) The following radicals were prepared using eq 1: (i-Pr$_3$Si)$_3$Si•, R(t-Bu$_2$MeSi)$_2$Si•(R = Ph; 2,4,6-trimethylphenyl; (Me$_3$Si)$_3$Si; (i-Pr$_3$Si)$_2$HSi). The synthesis and spectroscopy of these radicals will be reported elsewhere.

(8) See Supporting Information for the CIF file and experimental details (Figure S2).

(9) The EPR spectrum of **1** in toluene glass at 130 K (Figure S7) shows low anisotropy of the axial g-factor tensor ($g_\perp = 2.0068$, $g_\parallel = 2.0034$) and high anisotropy of the hyperfine coupling tensor with the ^{29}Si$^{\alpha}$ nuclei: $A_\perp \approx 0$ G, $A_\parallel$ (^{29}Si$^{\alpha}$) = 113 G.

(10) Radical **3** was synthesized by the reaction of (i-Pr$_3$Si)$_2$HSiSiCl$_2$H with i-Pr$_3$SiLi, i.e., using eq 1; see the Supporting Information.

(11) Weil, J. A.; Bolton, J. *Electron Paramagnetic Resonance*, 2nd ed.; John Wiley & Sons: Hoboken, NJ, 2007.

(12) (a) Stanislavski, D. A.; Buchanan, A. C., III.; West, R. *J. Am. Chem. Soc.* **1978**, *100*, 7791. (b) Sakurai, H.; Kira, M.; Sato, M. *Chem. Lett.* **1974**, *3*, 1323. (c) Jackson, R. A.; Rhodes, C. J. *J. Organomet. Chem.* **1987**, *336*, 45.

(13) Calculations were carried out at the UB3LYP/TZVP//UB3LYP/6-31G(d) level using the Gaussian 03, Revision D.02 series of programs: Frisch, M. J.; et al. *Gaussian 03*, revision D.02; Gaussian, Inc.: Wallingford, CT, 2004 (see the Supporting Information for the full list of authors and for the calculations' details).

(14) Krusic, P. J.; Kochi, J. K. *J. Am. Chem. Soc.* **1971**, *93*, 846.

(15) Disilene **4** was reported previously: Sekiguchi, A.; Inoue, S.; Ichinohe, M.; Arai, Y. *J. Am. Chem. Soc.* **2004**, *126*, 9626.

(16) (a) Takeda, N.; Kajiwara, T.; Suzuki, H.; Okazaki, R.; Tokitoh, N. *Chem.—Eur. J.* **2003**, *9*, 3530. (b) Gaspar, P. P.; West, R. In *The Chemistry of Organic Silicon Compounds*; Rappoport, Z., Apeloig, Y., Eds.; John Wiley & Sons: Chichester, U.K., 1998; Vol. 2.

(17) The experiment was carried out in the EPR tube upon irradiation with a 1 kW mercury lamp inside the cavity of an EPR spectrometer. Full conversion of **1** under these conditions occurs in 200 s. We note that the recorded second-order decay of **1** upon irradiation is not proof for the bimolecular reaction since the quantum yield of the reaction was not measured. The kinetic curves are given in Figure S8.

(18) In radical **2** *only* the SOMO-1 → SOMO transition occurs upon irradiation with λ > 400 nm. In radical **1** both SOMO-1 → SOMO and SOMO → LUMO transitions occur, and therefore photoexcited **1** may exhibit enhanced electron-donating properties (Figure S9).

(19) Heeger, A. J. *Rev. Mod. Phys* **2001**, *73*, 681.

(20) Related (not photoinduced) mechanism of hydrogen abstraction by organic radicals was reported: (a) Litwinienko, G.; Ingold, K. U. *Acc. Chem. Res.* **2007**, *40*, 222. (b) Mayer, J. M. *Annu. Rev. Phys. Chem.* **2004**, *55*, 363.

JA905097B